Journal of the Persian Gulf
(Marine Science)/Vol. 3/No. 10/December 2012/10/7-16

2DV Nonlinear *k-ε* Turbulence Modeling of Stratified Flows

Shams Nia, Hadi[1*]; Hejazi, Kuorosh

Dept. of Civil Engineering, K.N.Toosi University of Technology, Tehran, IR Iran

Received: July 2012 *Accepted: November 2012*

Abstract

The commonly used linear *k-ε* turbulence model is shown to be incapable of accurate prediction of turbulent flows, where non-isotropy is dominant. Two examples of non-isotropic flows, which have a wide range of applications in marine waters, are saline water flow and the stratified flows due to temperature gradients. These relate to stratification and consequently, variation of density through vertical layers. In this paper, a nonlinear *k-ε* turbulence model, firstly presented by Speziale (1987) and was implemented in the existing hydrodynamic model. The energy equation has been also added and solved in the hydrodynamic model. The hydrodynamic model solves the fully nonlinear Navier-Stokes equations based on an ALE (Arbitrary Lagrangian Eulerian) description. The model is an extension to WISE (Width Integrated Stratified Environments) 2DV numerical model, originally developed by Hejazi (2002). The simulated values have been compared with the experimental data and have shown acceptable agreements. The predictions are also compared with the results of the original model employing a standard buoyant k-ε turbulence model, which showed the advantage of the new turbulence model in prediction of non-isotropic flows.

Keywords: *Nonlinear k-ε, Non-Isotropic turbulence, Stratified flows, Temperature gradients, FVM.*

1. Introduction

Despite the intensive research efforts of the past decades to develop more general turbulence models, *k-ε* models, still remain the most widely used approach by engineers and scientists for the solution of practical problems. The main advantage of *k-ε* turbulence model is due to the reasonable computational time compared with the more complicated models.

To improve the predictions of k-ε turbulence model, a lot of research work has been carried out. Lumley (1970) developed a turbulent constitutive relation which was based on the similarities between non-Newtonian fluids and nonlinear Reynolds stress and mean strain relation. Pope (1975) presented a nonlinear *k-ε* turbulence model based on the Caley-Hamilton theorem and integrity basis tensors. An extensive research effort was carried by Speziale (1987) to enable turbulence modeling with consideration of anisotropy by the application of nonlinear *k-ε* models. One example, where anisotropy is dominant and widely applicable and important in geophysical, environmental and some other engineering turbulence flows, is stratified flow. The density variations due to stratification may be caused by heat transfer, salinity or other species concentration difference across the depth of flow. The flows, which lie in this category may

* *E-mail*: *hadishamsnia@sina.kntu.ac.ir*

increase or damp turbulence fluctuations depending on occurrence of stable or unstable shear layers, which are widely applicable in environmental marine flows. In stratified flows, stress induced anisotropy is present. Therefore, linear turbulence models may not result in accurate predictions of turbulence and hydrodynamics characteristics of such flows.

The new model has been simulated for three lock-release type tests, and also heated buoyant jets discharging into an ambient flow, for which the laboratory experimental values were reported in the literature. Velocity and concentration profiles have been compared with the measured values and linear *k-ε* model predictions.

2. Governing Equations

Continuity and conservative Navier-Stokes equations with the Reynolds stresses terms in ALE description (Eqs. 1, 2 and 3) have been deployed and implemented in the hydrodynamic model (WISE) originally developed by Hejazi (2002):

$$\frac{\partial u}{\partial x}+\frac{\partial w}{\partial z}=0 \tag{1}$$

$$\frac{\partial u}{\partial t}+\frac{\partial u^2}{\partial x}+\frac{\partial wu}{\partial z}=\frac{1}{\rho_r}X-\frac{1}{\rho_r}\frac{\partial p}{\partial x}+\frac{\partial}{\partial x}\left(v\frac{\partial u}{\partial x}\right)+\frac{\partial}{\partial z}\left(v\frac{\partial u}{\partial z}\right)+\frac{\partial \tau_{xx}}{\partial x}+\frac{\partial \tau_{xz}}{\partial z} \tag{2}$$

$$\frac{\partial w}{\partial t}+\frac{\partial uw}{\partial x}+\frac{\partial w^2}{\partial z}=\frac{1}{\rho_r}Z-\frac{1}{\rho_r}\frac{\partial p}{\partial z}+\frac{\partial}{\partial x}\left(v\frac{\partial w}{\partial x}\right)+\frac{\partial}{\partial z}\left(v\frac{\partial w}{\partial z}\right)-g\frac{\rho-\rho_r}{\rho_r}+\frac{\partial \tau_{xz}}{\partial x}+\frac{\partial \tau_{zz}}{\partial z} \tag{3}$$

where, x and z are the horizontal and vertical directions in Cartesian coordinate system, respectively, u and w the horizontal and vertical velocity components, respectively, p the pressure, ρ_r and ρ the reference density and density of the fluid, respectively, X and Z the body forces in the x and z directions, respectively, v the kinematic viscosity, g the gravitational acceleration, and τ_{xx}, τ_{xz} and τ_{zz} are the Reynolds stresses.

The tonsorial form of the representative equations for these stresses are as follows (Speziale, 1987):

$$\tau_{ij}=-\frac{2}{3}\rho k\delta_{ij}+\rho k^{\frac{1}{2}}l\bar{D}_{ij}+C_D\rho l^2\left(\bar{D}_{im}\bar{D}_{mj}-\frac{1}{3}\bar{D}_{mn}\bar{D}_{mn}\delta_{ij}\right)+C_{E\rho}l^2(\dot{\bar{D}}_{ij}-\frac{1}{3}\dot{\bar{D}}_{mm})\delta_{ij} \tag{4}$$

where, τ_{ij} is the Reynolds stress tensor, k the turbulent kinetic energy, l the turbulent length scale, ρ density, δ_{ij} the Kronecker delta, $\bar{D}_{ij}$ the mean strain tensor, $\dot{\bar{D}}_{ij}$ the Oldroyd derivative of mean strain tensor and, $C_D=C_E=1.68$ are constant coefficients. The Oldroyd derivative of mean strain tensor is defined as follows (Speziale, 1987):

$$\dot{\bar{D}}_{ij}=\frac{\partial \bar{D}_{ij}}{\partial t}+\bar{U}.\nabla\bar{D}_{ij}-\frac{\partial \bar{U}_i}{\partial x_k}\bar{D}_{kj}-\frac{\partial \bar{U}_j}{\partial x_k}\bar{D}_{ki} \tag{5}$$

where, $\bar{U}$ is the velocity vector and ∇ represents the gradient operation.

In the k-ε turbulence model, the length scale of turbulence model is taken to be of the form (Speziale, 1987):

$$l=C\frac{k^{\frac{3}{2}}}{\varepsilon} \tag{6}$$

where, C is a dimensionless constant.

k and ε transport equations are as follows (Rodi, 1993):

$$\frac{\partial k}{\partial t}+\bar{u}_i\frac{\partial k}{\partial x_i}=\frac{\partial}{\partial x_i}\left(\frac{v_t}{\sigma_k}\frac{\partial k}{\partial x_i}\right)+v_tP+\beta g_i\frac{v_t}{\sigma_t}\frac{\partial \emptyset}{\partial x_i}-\varepsilon \tag{7}$$

$$\frac{\partial \varepsilon}{\partial t}+\bar{u}_i\frac{\partial \varepsilon}{\partial x_i}=\frac{\partial}{\partial x_i}\left(\frac{v_t}{\sigma_\varepsilon}\frac{\partial \varepsilon}{\partial x_i}\right)+C_{1\varepsilon}\frac{\varepsilon}{k}(P+G)\left(1+C_{3\varepsilon}R_f\right) \tag{8}$$

where, v_t is the eddy viscosity, ∅ the concentration or temperature, P the production term, G the buoyancy term, R_f the Richardson number of the flow, σ_t the Schmitt number and, σ_k, β, σ_ε, $C_{1\varepsilon}$, $C_{3\varepsilon}$ are coefficients, which have been defined in Rodi (1993). For considering the near wall treatment, appropriate wall functions have been used (Rodi, 1993). The production term in nonlinear model is different from the linear model and is defined as follows:

$$\mathrm{p}=\tau_{xx}\frac{\partial u}{\partial x}+\tau_{xz}\left(\frac{\partial u}{\partial z}+\frac{\partial w}{\partial x}\right)+\tau_{zz}\frac{\partial w}{\partial z} \tag{9}$$

In this study, the linear form of production term (Rodi, 1993) has been used and discretized for the cells adjacent to the bed and the nonlinear form of

the production term has been used in the rest of domain.

The species concentration and temperature field equation also has been solved for salinity (Rodi, 1993) and temperature:

$$\frac{\partial \emptyset}{\partial t}+\bar{u}\frac{\partial \emptyset}{\partial x}+\bar{w}\frac{\partial \emptyset}{\partial z}=\lambda\frac{\partial^2 \emptyset}{\partial x^2}+\lambda\frac{\partial^2 \emptyset}{\partial z^2}-\frac{\partial}{\partial x}\left(\overline{u'\emptyset'}\right)-\frac{\partial}{\partial z}\left(\overline{w'\emptyset'}\right)+S_{\emptyset} \quad (10)$$

where, $\emptyset$ represents the temperature, salinity or other types of species concentration, λ is the diffusion coefficient, and $S_{\emptyset}$ is the source term. The terms $\overline{u'\emptyset'}$ and $\overline{w'\emptyset'}$ t are modeled. $\overline{u'\emptyset'}$, for instance uses the following relation:

$$\overline{u'\emptyset'}=\Gamma\frac{\partial \emptyset}{\partial x} \quad (11)$$

where, for salinity field, Γ is the turbulent diffusivity coefficient of concentration, and λ and Γ are defined as follows:

$$\lambda=\frac{\nu}{\sigma} \quad (12)$$

$$\Gamma=\frac{\nu_t}{\sigma_T} \quad (13)$$

in which, σ and σ_T are Schmidt number and turbulent Schmidt number respectively. For temperature field Γ is the turbulent diffusivity coefficient of temperature, and λ and Γ are defined as follows:

$$\lambda=\frac{\nu}{Pr} \quad (14)$$

$$\Gamma=\frac{\nu_t}{Pr_t} \quad (15)$$

in which, Pr and Pr_t are Prandtle number and turbulent Prandtle number respectively. State equation was used to calculate the density at each time step after the energy equation was solved.

3. Solution Method

WISE is a hydrodynamic free surface numerical model based on time-dependent Reynolds-averaged Navier-Stokes equations. The model is capable of handling problems involving vertical flow characteristics and environmental variations including complex bathymetries. A structured non-orthogonal curvilinear staggered mesh is used for computational domain, based on Arbitrary Lagrangian-Eulerian description. The discretization of the flow and transport equations is based on finite volume method, providing flexibility for defining control volumes in a staggered grid system. The solution method is based on a fractional step scheme, whereby the problem is solved by time-splitting the set of governing conservation equations, which resembles a projection method.

The discretization and solution of the new turbulence model equations are the same as hydrodynamic model scheme. Reynolds stresses have been computed using central difference scheme for second and third order derivatives of velocity, while for the first order derivatives of velocity, finite volume method for each grid, has been employed. The Reynolds stresses play as source terms in the momentum equations. The tonsorial form of equation (4) for one of the Reynolds stresses, τ_{xz} for instance, may be spread as follows:

$$\tau_{xz}=\rho C_\mu\frac{k^2}{\varepsilon}\left(\frac{\partial u}{\partial z}+\frac{\partial w}{\partial x}\right)-4\rho C_E C_\mu{}^2\frac{k^3}{\varepsilon^2}\left(\frac{\partial u}{\partial z}\frac{\partial w}{\partial z}+\frac{\partial u}{\partial x}\frac{\partial w}{\partial x}\right)+2\rho C_E C_\mu{}^2\frac{k^3}{\varepsilon^2}\left(u\left(\frac{\partial^2 w}{\partial x^2}-\frac{\partial^2 w}{\partial z^2}\right)\right)+2\rho C_E C_\mu{}^2\frac{k^3}{\varepsilon^2}\left(w\left(\frac{\partial^2 u}{\partial z^2}-\frac{\partial^2 u}{\partial x^2}\right)\right)+\frac{\partial}{\partial t}\left(\frac{1}{2}\left(\frac{\partial u}{\partial z}+\frac{\partial w}{\partial x}\right)\right) \quad (15)$$

where, t represents the time.

Equation (16) is discretized as follows:

$$\tau_{xz}=\rho C_\mu\frac{\left(k_{i,k}^n\right)^2}{\left(\varepsilon_{i,k}^n\right)}\left(\frac{\partial u}{\partial z}+\frac{\partial w}{\partial x}\right)^n-4\rho C_E C_\mu{}^2\frac{(k_{i,k}^n)^3}{(\varepsilon_{i,k}^n)^2}\left(\frac{\partial u}{\partial z}\frac{\partial w}{\partial z}+\frac{\partial u}{\partial x}\frac{\partial w}{\partial x}\right)^n+2\rho C_E C_\mu{}^2\frac{\left(k_{i,k}^n\right)^3}{\left(\varepsilon_{i,k}^n\right)^2}\left(u\left(\frac{\partial^2 w}{\partial x^2}-\frac{\partial^2 w}{\partial z^2}\right)+w\left(\frac{\partial^2 u}{\partial z^2}-\frac{\partial^2 u}{\partial x^2}\right)\right)^n+\left(\frac{1}{2}\left(\frac{\partial u}{\partial z}+\frac{\partial w}{\partial x}\right)\right)^n-\left(\frac{1}{2}\left(\frac{\partial u}{\partial z}+\frac{\partial w}{\partial x}\right)\right)^{n-1} \quad (16)$$

The discretization of $\frac{\partial u}{\partial z}$, $\frac{\partial w}{\partial x}$, $\frac{\partial^2 w}{\partial x^2}$, and $\frac{\partial w}{\partial z}$, for instance, have been presented in equations (18) to (21) respectively.

$$\left(\frac{\partial u}{\partial z}\right)^n = \frac{\left(u^n_{i-1,k+2}+u^n_{i+1,k+2}-u^n_{i-1,k-2}-u^n_{i+1,k-2}\right)}{\left(4\Delta z_{i,k}\right)} \quad (18)$$

$$\left(\frac{\partial w}{\partial x}\right)^n = \frac{1}{A_{cell}}\left(w^n_{i,k+1}\left(z_{i+1,k+1}-z_{i-1,k+1}\right)-\right.$$

$$w^n_{i,k-1}\left(z_{i+1,k-1}-z_{i-1,k-1}\right)+ \quad (19)$$

$$\left.+\frac{1}{4}\left(w^n_{i+2,k+1}+w^n_{i,k+1}+w^n_{i,k-1}+w^n_{i+2,k-1}\right)\left(\Delta z_{i+1,k}\right)-\right.$$

$$\left.\frac{1}{4}\left(w^n_{i-2,k+1}+w^n_{i,k+1}+w^n_{i,k-1}+w^n_{i-2,k-1}\right)\left(\Delta z_{i-1,k}\right)\right)$$

$$\left(\frac{\partial^2 w}{\partial x^2}\right)^n = \frac{\left(w^n_{i-2,k-1}+w^n_{i-2,k+1}-2\left(w^n_{i,k-1}+w^n_{i,k+1}\right)+w^n_{i+2,k-1}+w^n_{i+2,k+1}\right)}{\left(4(\Delta x)^2\right)} \quad (20)$$

$$\left(\frac{\partial w}{\partial z}\right)^n = \left(w^n_{i,k+1}-w^n_{i,k-1}\right)/\left(\Delta z_{i,k}\right) \quad (21)$$

The Reynolds stresses derivatives are also discretized in a similar manner and are considered as source terms into diffusion terms where the diffusion is computed in the hydrodynamic model.

4. Results and Discussion

4.1. Saline Water

In order to investigate and compare the results of the nonlinear *k-ε* turbulence model, the simulation results have been compared with the measured values of three experimental studies of lock-release type and corresponding predicted values of linear buoyant *k-ε* turbulence model.

The first test was based on the experimental study accomplished by Zhu et al. (2006) as a lock-release type of gravitational flows. The experiments were carried out in a rectangular perspex flume, 200 mm wide, 400 mm deep and 2590 mm long. The flume was filled with fresh water to a depth of H_0 = 100 mm and a perspex gate were positioned vertically at a distance of x_0 = *200 mm* away from the left end of the channel to form a lock. Salt was dissolved into the water behind the perspex gate to create a density difference $\Delta\rho$ between the two parts of the flume. The densities of saline water ($\rho_0 = 1009.5 kg/m^3$) and fresh water ($\rho_a = 999.5 kg/m^3$) were measured, corresponding to a density difference of $\Delta\rho = \rho_0 - \rho_a = 10.0\ kg/m^3$.

Figure 1 shows the gravitational current simulations for linear buoyant and nonlinear *k-ε* models of turbulence, compared with the front head position reported in the experimental measurements conducted by Zhu et al. (2006).

During an initial slumping phase, the front head position x_f, increases linearly with time. Two distinct phases of lock-release front propagation were observed and at about 10 lock lengths, the transition from the first to the second phase occurs (Zhu et al., 2006).

Figure 2 shows the front head of the gravitational current versus time for nonlinear and standard buoyant *k-ε* turbulence models and measured values in a non-dimensional form. $x_f^* = x_f/x_0$, and $t^* = t/t_c$, where $t_c = x_0/\left(g\acute{H}_0\right)^{1/2}$, and $g = g\acute{}\Delta\rho/\rho_a$, in which x_0 is the lock length, H_0 the saline water depth, ρ_a the ambient flow density, t the time, g the gravity acceleration and x is the distance from upstream. While in the second phase of the gravitational flow extent, linear *k-ε* turbulence model predicts the front head better than non-linear model; both models overestimate the front head, in the first phase. The underestimation of nonlinear *k-ε* turbulence model may be due to its diffusive nature.

Figure 3 shows the velocity profiles of linear and nonlinear *k-ε* turbulence models in comparison with measured values at different locations, and at t=12.28s. It is evident that nonlinear *k-ε* turbulence model shows closer predictions.

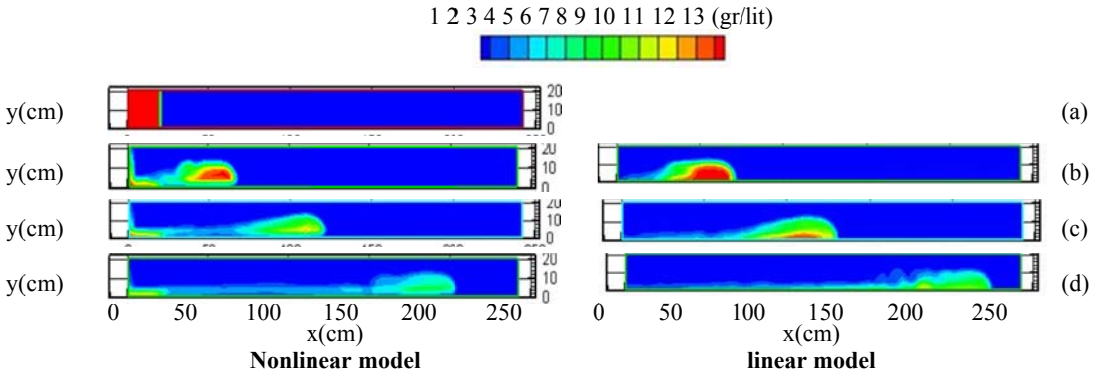

Fig.1: Gravitational flow simulation for linear and nonlinear models. (a) t=0, (b) t=35s, (c) t=80s, (d) t=160s

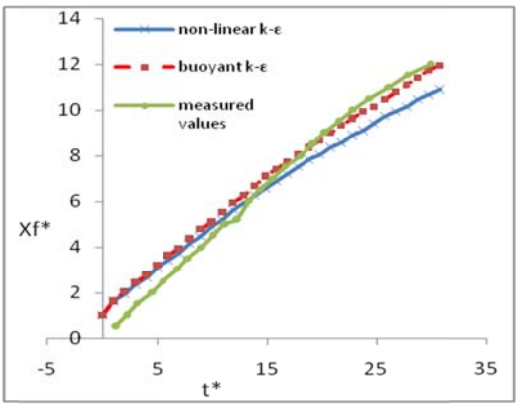

Fig. 2: Comparison of the front head position for measured values and simulations

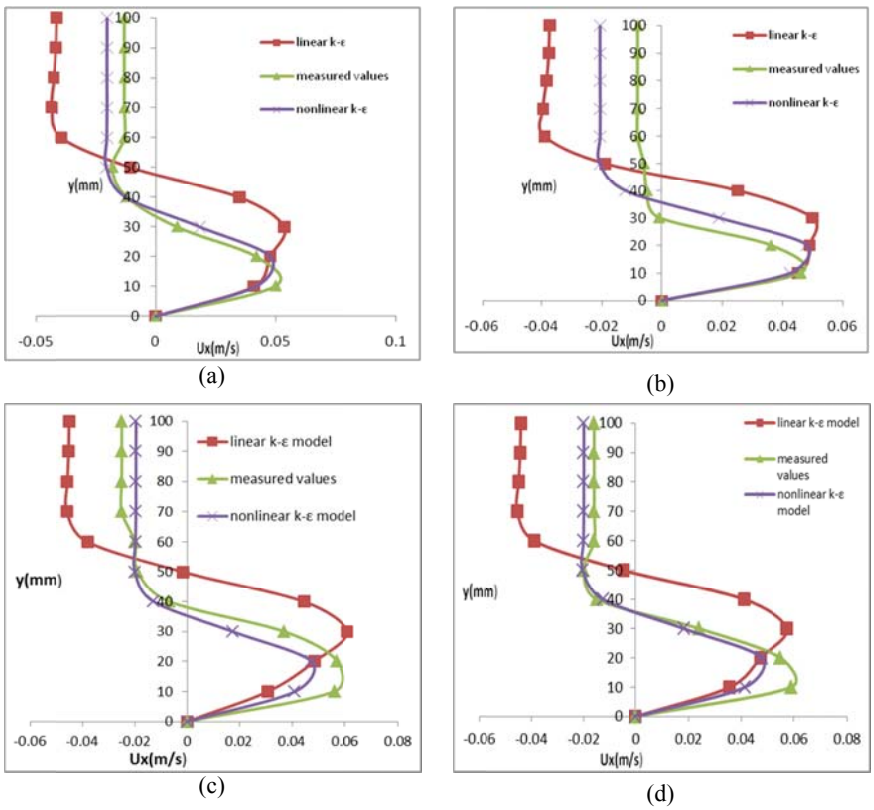

Fig. 3: Velocity profiles of linear and nonlinear *k-ε* turbulence models versus measured values: (a) x=1020mm, (b) x=1040mm, (c) x=1060mm, and (d) x=1080mm

The second test is based on the experimental data reported by Kneller et al. (1999).

The experimental procedure is somehow the same as the previous test, except for the distance between the lock and left end of the channel, which is 0.34 m, and a higher density difference of 41 kg/m^3. Figure 4 shows the velocity profile comparison of two models with measured values at *x=800mm* and *t=14s*. Y is the depth of the flow, at each point and Y_d the total depth of the flow. Acceptable agreement has been obtained for both models.

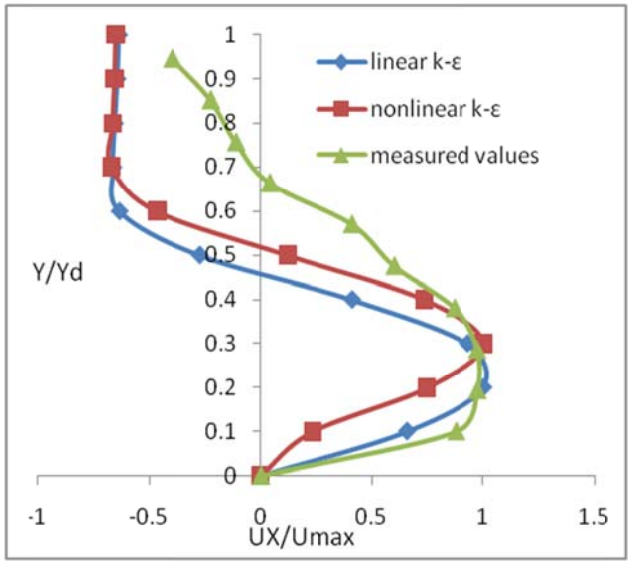

Fig. 4: Velocity profile comparison of linear and nonlinear *k-ε* models at x=0.8m and t=12s against measured values

As the third test of the lock-release type of stratified saline water, the predictions of the linear and nonlinear models have been compared with the experimental work accomplished by Herbert and Simpson (1980).

The experiment procedure is somehow the same as previous ones. The water depth is 0.1 m, the length of the lock, 0.39 m, and the density difference of fresh and saline water has been 9 kg/m^3. Figure 5 shows the front head of the gravitational current and shows an acceptable agreement for the nonlinear model, especially in the second phase of extension, while, the linear turbulence model provides closer predictions.

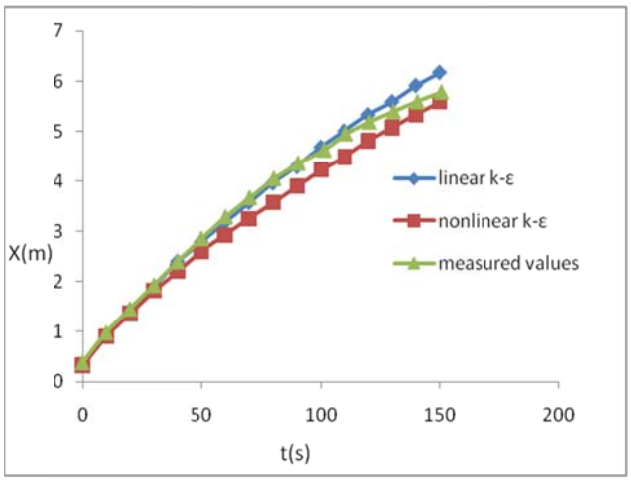

Fig. 5: Front head position of the gravitational flow

4.2. Temperature Gradient

The first test is based on the experimental data reported by Schiller et al. (1973), which was carried by Schiller and Sayre (1973). They ran a series of experiments in a flume with ambient water flow where, a spreader had been set on the water free surface to inject the hot water into the ambient flow horizontally. The flume was 85 ft long and 2.5 ft wide. The spreader was placed at a distance of 16.5 ft from the channel upstream, and provided a constant discharge. A comparison of the velocity and temperature profile, are presented herein. The ambient flow velocity was 0.5 ft/s, the flow depth was 0.25 ft, and the temperature difference between the jet and the ambient flow was 25 degrees of Fahrenheit for the first test and the corresponding values for the second test were 0.3 ft/s, 0.25 ft, and 5 degrees of Fahrenheit, respectively. Velocity comparisons are presented in Figure 6 for the first test, in which *d* is the flow depth, y the vertical distance from the bottom, and u_x the horizontal velocity, which showed closer predictions for the nonlinear *k-ε* turbulence model. Figure 7 shows the temperature profile for the second test, in which *T* is the temperature, T_{amb} the ambient flow temperature, *d* the flow depth, and *dt* the temperature difference

between the jet and ambient flow. At the water free surface both models predicted the velocity and temperature more inaccurately, while the nonlinear turbulence model provided closer predictions except for $x/d = 150$ in the first test. The larger values of discrepancies at the water surface might be due to excess turbulence caused by the spreader and hot water injection into the flume.

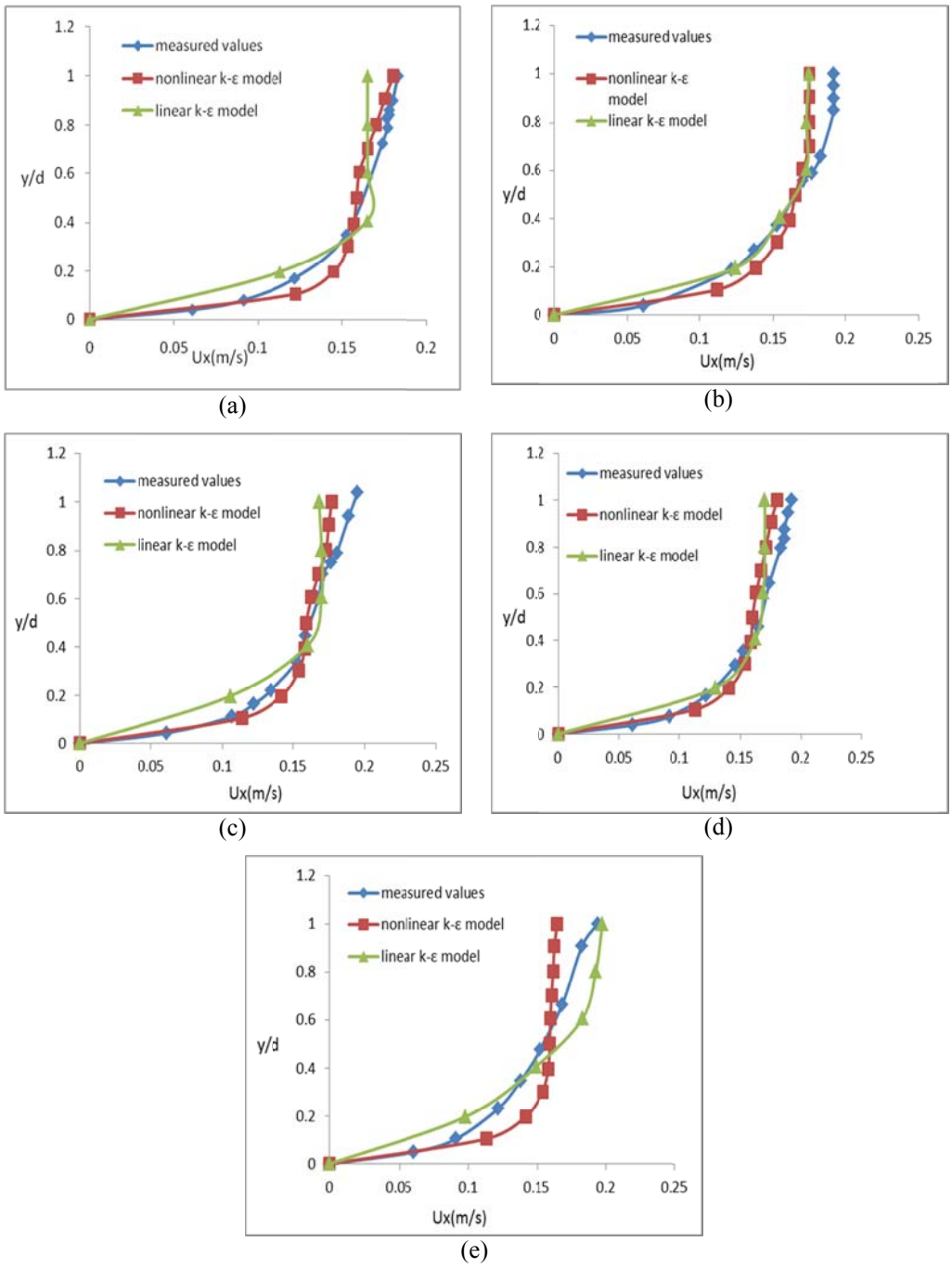

Fig. 6: Velocity profile comparison at (a) x/d=20, (b) x/d=40, (c) x/d=65, (d) x/d=100, and (e) x/d=150, at the distances measured from the spreader

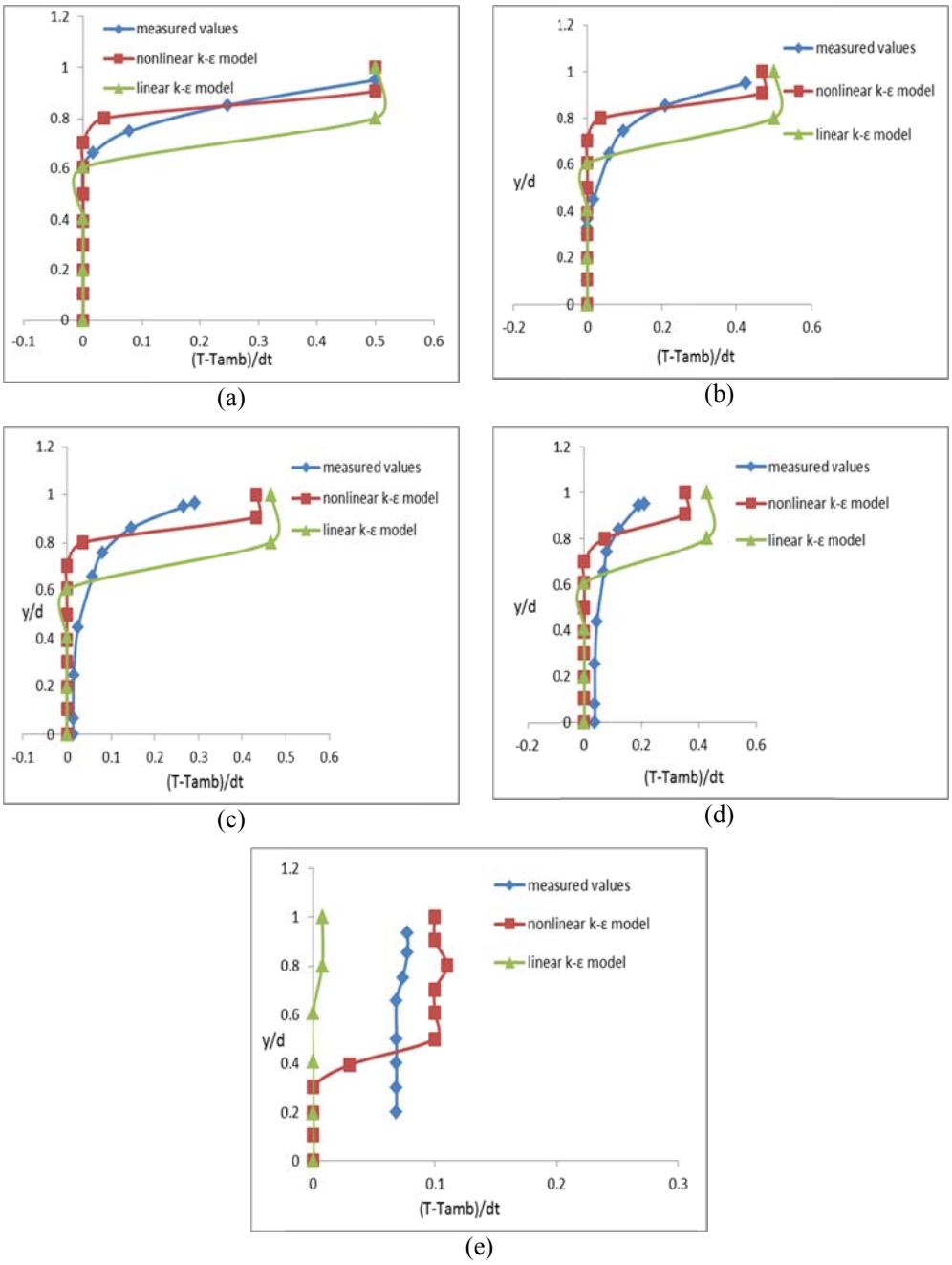

Fig. 7: Temperature profile comparison at (a) x/d=4, (b) x/d=12, (c) x/d =30, (d) x/d=50, (e) x/d=90 at the distances measured from the spreader

Ramaprian and Haniu (1983) conducted a series of tests on heated impinging jets into horizontal cross flows. The tests were the heated jet impinging into the horizontal ambient cross flow through the bottom. In this test, U_a is the horizontal flow velocity, U_j vertical velocity of the jet, dt the temperature difference between the flow and the mean flow, dt_j the temperature difference between the jet and the mean flow, d the jet diameter, x the vertical direction, and y is the horizontal direction. Two tests conditions were applied to compare the model predictions with results of Ramaprian and Haniu (1983). In the first test, dt_j sets as zero, $U_a = 0.05\ m/s$ and $U_j = 0.3\ m/s$ and the corresponding values for the second test, are $dt_j = 20$, $U_a = 0.01\ m/s$ and $U_j = 0.1\ m/s$. Figure 8 presents the vertical velocity which was normalized for the jet

velocity, against the normalized distance from the jet for the flow depth in the first test conditions, where x/d sets as 5. It is obvious from the figure that the nonlinear model provides better results for the vertical velocity while, the linear model underpredicts the vertical velocity.

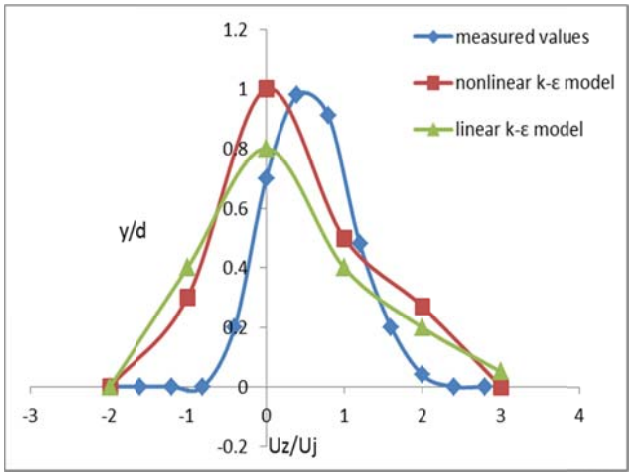

Fig. 8: Vertical velocity against the normalized horizontal direction at x/d=5

Figures 9 (a) and (b) present the normalized vertical velocity for the jet velocity and the normalized temperature difference of the flow for dt_j against the normalized vertical distance from the jet for the flow depth, respectively in the second test conditions. Here y/d sets as 40. Both models provided acceptable agreements with the experimental measurements, while the nonlinear turbulence model presented more accurate predictions than the linear model, when the temperature difference was set as zero.

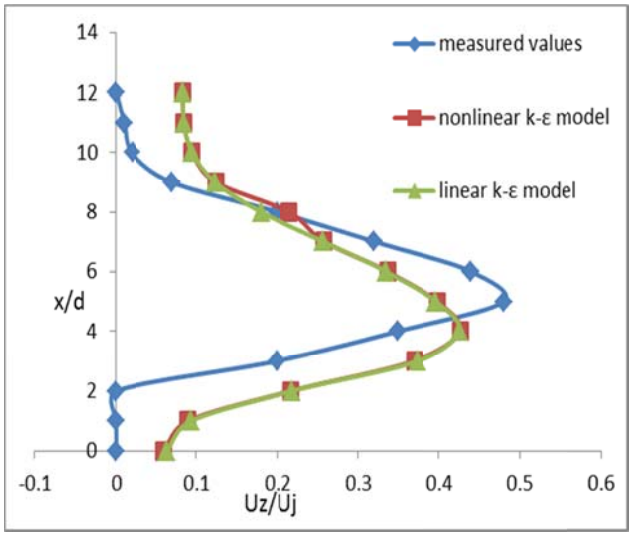

(a)

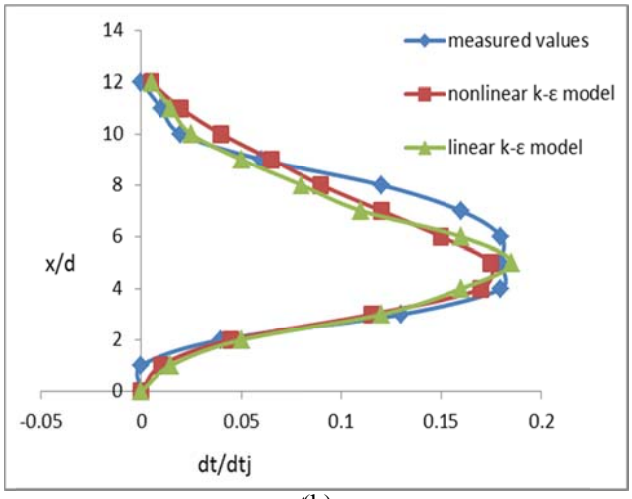

(b)

Fig. 9: Normalized vertical velocity (a) and normalized temperature difference (b) against the normalized vertical direction at y/d=40

5. Conclusion

In stratified saline water of lock-release types, the nonlinear model provided better results for velocity profiles especially near the bed. This occurred in both tests of Zhu et al. (2006) and Kneller et al. (1999). This meant that the nonlinear turbulence model was more reliable in prediction of the velocity field of lock-release types of stratified flows and it might be due to the effect of the turbulence closure equation accuracy on the velocity field in Navier-Stokes equations.

Both models provided acceptable predictions for the front head position. The underestimation was not of high importance, because of its low magnitude. The linear turbulence model provided more accurate results for the front head position in both phases of the gravitational flow extension in the tests carried by Zhu et al. (2006).

Therefore, it might be concluded that the linear model had a better function in predicting the front head position.

The comparisons of the results of linear and nonlinear turbulence models in the tests carried by Schiller et al. (1973), showed that both models provided rather acceptable predictions for horizontal velocity profiles while the nonlinear model presented closer predictions near the bed. The nonlinear turbulence model provided closer predictions to the

measurement values, than the linear turbulence model in most parts of the experiments. So, the nonlinear model could be considered more reliable in predictions of the velocity profiles in stratified flows due to temperature gradient.

Both models provided worse results near the free surface due to anisotropy and more extensive mixing, which were present near the free surface especially in near field. The nonlinear model presented more accurate results in some cases, because it was more capable of including the anisotropic features of the turbulent flows.

Both models presented coarser predictions for temperature profiles in far field rather than the near field. This might have occurred due to more extensive mixing, anisotropic nature of the flow, and high rate of momentum which existed, while the nonlinear turbulence model presented better results than the linear model even in far field and was more capable of predicting the mixing extension through the depth.

In the second test of the stratified flows with temperature gradients, both turbulence models had somehow similar predictions of the horizontal velocity profiles and temperature in the existence of the temperature difference between the jet and cross flow, while in the absence of the temperature difference, the nonlinear turbulence model had prsented more accurate predictions evidently.

Because the nonlinear turbulence model provided better results in most parts of the stratified flows of both models, while computational costs were not considerably greater than the cost of linear model, it could be concluded that stratified flows using nonlinear turbulence model was reasonable and suggested ,hereby. The only part in which the nonlinear model had worse predictions than the linear turbulence model, was the prediction of the front head position of gravitational flow in stratified flows of lock-release type.

Refferences

Hejazi., K., 2004. 3D Numerical modelling of flow and turbulence in oceanic water bodies using an ALE projection method. The First Seminar on Computer Simulation in Civil Engineering K.N.T.University: 47-99

Huppert, E.H. and Simpson, E.J., 1980. The slumping of gravity currents. Journal of Fluid Mechanics. 99 (4): 785-799

Kneller, B., Bonnett, S. and McCaffrey, W., 1999. Velocity structure, turbulence and fluid stresses in experimental gravity currents. Journal of Geophysical Research. 104 (C3): 5381-5391

Lumley, J. L., 1970. Toward a turbulent constitutive relation. Journal of Fluid Mechanics. 41 (2): 413-434

Pope, S.B., 1975. A more general effective-viscosity hypothesis. Journal of Fluid Mechanics. 72 (2): 331-340

Ramaprian, B.R., Haniu, H., 1983. Turbulence measurements in plane jets and plumes in cross-flow. Report No. 266, Iowa Institute of Hydraulic Research, University of Iowa. 347 P.

Rodi, W., 1993. Turbulence Models and their Application in Hydraulics. IAHR, 104 P.

Schiller, E.D. and Sayre, W.W., 1973. Vertical Mixing of Heated Effluents in open- Channel Flow. Report No. 148, Iowa Institute of Hydraulic Research, University of Iowa, Iowa City, Iowa. 125 P.

Speziale, C. G., 1987. On nonlinear k-l and k-ε models of turbulence. Journal of Fluid Mechanics, 178: 459-475

Zhu, J.B., Lee, C.B., Chen, G.Q., and Lee, J.H.W., 2006. PIV observation of instantaneous velocity structures of lock release gravity currents in the slumping phase. Communications in Nonlinear Science and Numerical Simulations. 11: 262-270.